Available online at www.sciencedirect.com
ScienceDirect
International Journal of Heat and Mass Transfer 51 (2008) 2020–2028
International Journal of HEAT and MASS TRANSFER
www.elsevier.com/locate/ijhmt

Heat transfer from immersed vertical tube in a fluidized bed of group A particles near the transition to the turbulent fluidization flow regime

A. Stefanova, H.T. Bi, C.J. Lim, J.R. Grace *

University of British Columbia, Department of Chemical and Biological Engineering, 2360 East Mall, Vancouver, Canada V6T 1Z3

Received 7 July 2006
Available online 6 August 2007

Abstract

Experiments were performed in a 0.29 m ID fluidization column to investigate heat transfer from a vertical tube immersed in a bed of 70 μm FCC particles in the range of superficial velocities close to the transition to the turbulent fluidization regime. The results show that the transition is a gradual process and that the changing hydrodynamics affect the heat transfer. The highest heat transfer coefficients were found in the range of superficial gas velocities where the transition to turbulent regime occurred. Radial profiles of heat transfer coefficient were almost flat in the turbulent fluidization regime and changed very little with increasing superficial gas velocity.

1. Introduction

Three modes of heat transfer are important with respect to surfaces immersed in fluidized beds: (1) convection by particles carrying heat conducted through the gas layer in contact with the exchange surface; (2) convection by gas, and (3) radiation. Many processes utilizing fluidized beds operate at temperatures below 500 °C where the radiation component is of secondary significance [1]. For the processes listed in Table 1 [2,3], the main interest is the convective heat transfer component. The particles used in these processes belong to Geldart group A, and the superficial gas velocities are relatively high, as shown in Table 1. Experience in operating these units has shown that increased gas velocities lead to a more homogeneous flow structure, improved mixing and high heat transfer rates. These are features of the turbulent fluidization flow regime, a transitional regime situated between bubbling and fast fluidization.

The development of a probabilistic fluidized bed reactor model [4] highlights the need for a heat transfer model that can be applied across different fluidization flow regimes, in particular bubbling, turbulent and fast fluidization. Heat transfer in bubbling and fast fluidization has been studied extensively (see the recent review by Chen [5]), but little work has been done on heat transfer in the turbulent fluidization regime. Comparison of different heat transfer correlations in the literature and experimental data for bubbling beds shows deviations of the order of 100% [6]. One reason for such large deviations is that some of the beds were actually in the turbulent fluidization flow regime and that the change in hydrodynamics accompanying the transition to the turbulent regime was not considered.

Very few experimental studies on heat transfer report explicitly on whether the bed was operated in the turbulent fluidization regime [7–13], though there are undoubtedly studies in the literature where the hydrodynamic regime was not determined, but where the turbulent flow regime was present. Except for the studies of Leu et al. [10] and Sun and Chen [13], the particles have been relatively large. Sun and Chen [13] and Basu et al. [7] reported that their maximum heat transfer corresponded closely to the onset of the turbulent flow regime. A lack of studies of heat transfer in turbulent fluidization regime is likely associated, to some extent at least, with uncertainties regarding the onset of the turbulent regime.

Given the advantage of operating at or near the maximum heat transfer coefficient in processes where heat

* Corresponding author. Tel.: +1 604 822 3121; fax: +1 604 822 6003.
E-mail address: jgrace@chml.ubc.ca (J.R. Grace).

0017-9310/$ - see front matter © 2007 Elsevier Ltd. All rights reserved.
doi:10.1016/j.ijheatmasstransfer.2007.06.005

Nomenclature

A_s	heat exchange surface area, m^2
Cr	correlation coefficient employed by Wender and Cooper [24]
D_t	column diameter, m
H	expanded bed height, m
h	heat transfer coefficient, W/m^2 K
H_0	static bed height, m
I	electrical current, A
Nu	Nusselt number, $Nu = hd_p/k_g$
Q_l	heat losses, W
R	column radius, m
R'	reduced column radius ($R' = R - r_t$), m
Re_p	Reynolds number, $Re_p = Ud_p\rho_g/\mu_g$
r	distance from column axis to heater axis, m
r_t	radius of heater tube, m
T_b	bed temperature, °C
T_s	surface temperature, °C
U	superficial gas velocity, m/s
U_c	velocity at onset of turbulent regime, m/s
U_{mf}	minimum fluidization velocity, m/s
V	voltage, V
x_i	fraction of particles having diameter d_{pi}
Δp	differential pressure, kPa
Δz	axial distance between pressure taps, m

Greek symbols

ε_0	packed bed voidage, –
κ	dimensionless constant introduced by Martin [26], $\kappa = 2$–4
ρ_p	particle density, kg/m^3

Table 1
Some commercial turbulent fluidized bed reactors operating at temperatures below 500 °C [2,3])

Process or product	Particle classification	Typical gas velocity (m/s)	Temperature range (°C)
Mobil MTG reactors	Group A	~0.5	400–500
Acrylonitrile	Group A	0.4–0.7	400–500
Maleic anhydride	Group A	~0.5	400–500
Phthalic anhydride	Group A	0.3–0.6	340–385
Chlorination of methane	Group A	~0.5	350–400
Ethylene dichloride	Group A	~0.5	~270

transfer is important, it is clearly of value to investigate, understand and model heat transfer in this flow regime, and this will be the subject of a future publication. The research in this paper is focused on an experimental investigation of convective heat transfer coefficients from an immersed vertical tube in a cold model fluidized bed of Geldart group A particles over a range of velocities where the bed undergoes a transition from the bubbling to the turbulent fluidization flow regime. The effects of gas velocity, radial position of the heat exchanger tube and bed depth are reported.

2. Experimental methods

2.1. Equipment and instrumentation

The heat transfer experiments were performed in a 0.29 m ID, 4.5 m high Plexiglas fluidization column as shown schematically in Fig. 1. Air was supplied by a positive displacement Roots blower (1), with a maximum flow of 425 Nm^3/h (0.118 Nm^3/s) at 69 kPa. The air flow to the column was controlled by a ball valve in the bypass line (2) and measured by means of an orifice plate (3). The air passing through the windbox (4) was distributed by a perforated distributor plate (5) consisting of two perforated plates, each with 98 aligned holes in an equilateral triangular pattern with centres 32 mm apart. To prevent the particles from falling through the holes, a 38-μm stainless steel mesh was sandwiched between the two plates. The column (6) had 59 side ports (7 and 8 on Fig. 1) on opposite sides of the column for pressure and temperature measurements. Particles entrained from the column through the abrupt exit were collected by two cyclones. The primary cyclone (9a) discharged the solids into the primary return leg (10). Fine solids and gas leaving the top of the primary cyclone entered the secondary cyclone (9b) where more solids were collected and returned to the bed via a secondary return leg (10). Each of the return legs was equipped with a butterfly valve (11). The two return legs merged together before connecting to a section equipped with a flapper valve (12), controlling the particle return flow to the bed by pressure balance. The exit from the secondary cyclone was connected through a bag house filter (13) to the ventilation system.

An electrically heated tube (14) was designed and manufactured to measure the heat transfer coefficients. Ni–Cr heating wire was wound around a hollow cylindrical Teflon core, and this assembly was inserted in a copper shell (0.0286 m OD and 0.101 m long) to obtain an even temperature distribution and smooth surface. The space between the heater and the heating wire was filled with thermally conductive cement. Care was taken to prevent any air from being trapped inside. At the tube ends, Teflon pieces of semi-spherical shape (15) were installed to minimize heat

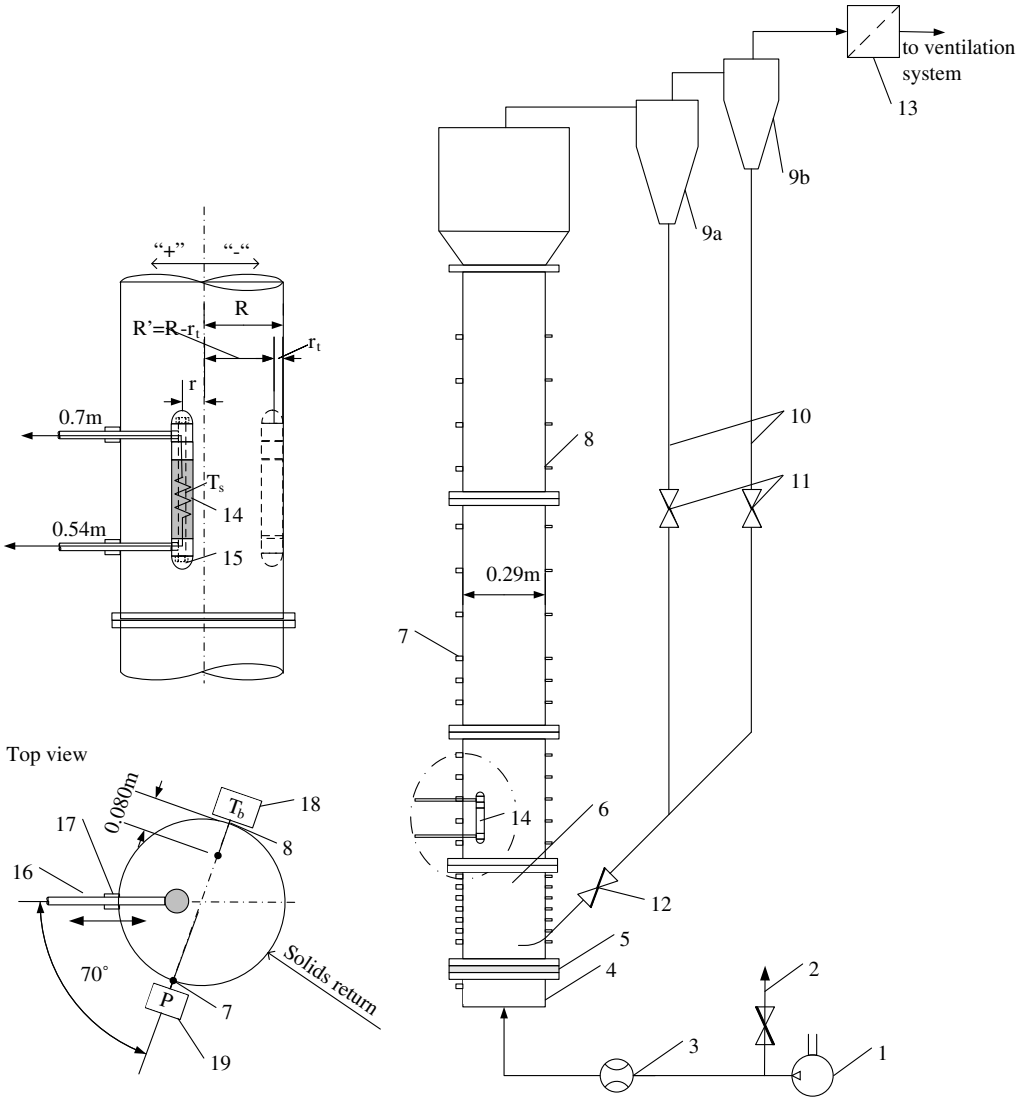

Fig. 1. Experimental set-up. 1: blower; 2: bypass line; 3: orifice plate; 4: windbox; 5: distributor; 6: column; 7: 1/2 NPT ports; 8: 1/4″ NPT ports, 9a and b: cyclones; 10: return leg; 11: valve; 12: flapper valve; 13: bag house filter; 14: heater; 15: Teflon caps; 16: support arms; 17: 3/4″ ports; 18: thermocouples; 19: pressure sensors.

losses. Two T-type thermocouples were installed on the heater surface to measure the surface temperature. Two other T-type thermocouples were installed near the tube ends. The heater tube was supported and positioned at different radial locations by two horizontal tubes (16) (Fig. 1). All wires were led through the hollow heater core and then through the support tubes to the data acquisition system and the power supply. Power to the heater was supplied by a DC power source, Samlex PSA 305, with adjustable voltage.

The heat transfer coefficient, h was calculated from:

$$h = \frac{VI - Q_l}{A_s(T_s - T_b)} \tag{1}$$

The voltage V and current I supplied to the heater were logged to the data acquisition system using a voltage divider and current sensor, respectively. Heat losses, Q_l, were estimated by comparing the experimental data obtained for the heater tube in an air flow with correlations for forced and free air convection [14] from vertical surfaces. The total heat loss was found to be in the range 2–4% for heat transfer coefficients of 100–400 W/m^2 K. The overall uncertainty of the measured heat transfer coefficient, including the heat losses, is estimated to be ±4.5% [15]. Bed temperature T_b was measured by five T-type thermocouples (18) positioned along the height of the bed (Fig. 1). The axial profile of temperature was quite uniform, and the arithmetic mean was taken as the bed temperature T_b. The heater surface temperature, T_s was calculated as the arithmetic mean of the temperatures measured by the T-type thermocouples attached to the heater surface.

Information on the hydrodynamics of the bed was obtained from pressure measurements based on eleven differential and seven absolute pressure sensors, 142PC series, connected to pressure taps (19) located along the column,

Table 2
Bed material properties

Particles	d_p (μm)	ρ_p (kg/m^3)	c_p (J/kg K)	ε_0 (–)	U_{mf} (m/s)
FCC	70	1600	800	0.45	0.0025

flush with the column wall (Fig. 1). Standard deviations of pressure fluctuations were acquired from the dynamic measurements, giving information on the transition to the turbulent flow regime. Bed expansion, mean bed voidage and cross-sectional mean bed voidage were obtained from the steady state pressure measurements. The mean bed voidage was calculated from the momentum balance, assuming that the pressure drop across the expanded bed height is equal to the weight of the bed per unit area. The uncertainty of the voidage calculated in this manner was estimated to be ±2.5% [15].

All instruments (pressure transducers, thermocouples, current sensors) were connected to an analog/digital converter (DAS08) and then to a PC via 32-channel expansion boards. Once steady state was achieved, data were recorded every 5 s for 5–10 min using a custom-made Visual Basic program. The pressure fluctuation data were recorded for periods of 100 s at a sampling frequency of 50 Hz using Labtech Notebook software.

2.2. Bed material

The properties of the spent fluid cracking catalyst (FCC) particles used in the experiments are provided in Table 2. Sieve analysis was performed to obtain the particle size distribution and mean diameter. The mean particle diameter d_p was calculated as:

$$d_p = \frac{1}{\sum \frac{x_i}{d_{pi}}} \tag{2}$$

where x_i is the mass fraction of particles having diameter d_{pi}. The particle density ρ_p was obtained from the supplier.

3. Results and discussion

3.1. Transition velocity, U_c

The superficial gas velocity marking the onset of the transition to the turbulent fluidization flow regime, U_c, is commonly defined as the velocity at which the standard deviation of pressure fluctuations reaches a maximum. Chen and Bi [16] showed that the maximum of the standard deviation of pressure fluctuations corresponds to either the maximum bubble size or to a reduction of the separation distance between bubbles, providing a mechanism for transition to the turbulent regime.

Differential and absolute pressure fluctuations were recorded at different axial locations along the column. Third-order polynomial curves with superficial gas velocity as the abscissa were least-square-fitted through the standard deviation of pressure fluctuations for each axial position, and the maximum of each curve was then determined in the range of superficial gas velocities from 0.1 to 1 m/s. This procedure was performed for both absolute and differential pressure fluctuations for each static bed height, H_0, investigated. The results confirm that the transition to the turbulent regime is a gradual process, starting from the top of the bed and progressing to the bottom as the gas velocity is increased, as previously reported by Ellis [17]. The transition is also affected by static bed height for $H_0/D_t < 3$, deeper beds giving higher U_c. The data from the absolute and differential pressure transducers located close to the level of the heater (0.45–0.75 m above the distributor plate) were used to determine the range of transition velocities U_c for comparison with the heat transfer data. Fig. 2 shows the standard deviation of absolute pressure fluctuations (AP) 0.464 m and 0.654 m above the distributor plate and of differential pressure fluctuations (PD) 0.591 m above the distributor plate (axial distance between ports, $\Delta z = 0.127$ m), for a static bed height $H_0 = 0.8$ m. U_c was found to be in the range 0.46–0.65 m/s for $H_0 = 0.8$ m and 0.6–0.8 m/s for $H_0 = 1.0$ and 1.2 m.

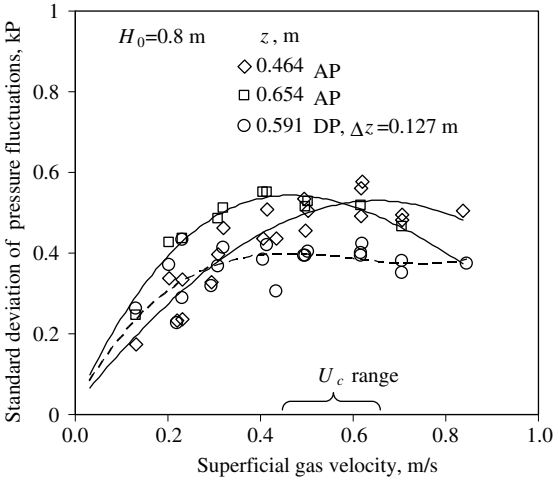

Fig. 2. Standard deviation of pressure fluctuations for $H_0 = 0.8$ m; AP: absolute pressure, DP: differential pressure. U_c lies in the range 0.46–0.65 m/s.

3.2. Effect of gas velocity

The measured heat transfer coefficients with increasing gas velocity for H_0=0.8 m are plotted in Fig. 3 for a vertical tube located at the axis of the bed. The range of velocities corresponding to the transition to the turbulent fluidization regime is indicated on the figure. The error bars represent ± one standard deviation of the signal. Below U_c, in the bubbling regime, the heat transfer coefficient increased with increasing gas velocity. In the range of velocities where the onset on turbulent fluidization was observed, the heat transfer coefficient reached a shallow maximum, after which it slightly decreased for the static bed height $H_0 = 0.8$ m. The decrease of the heat transfer coefficient

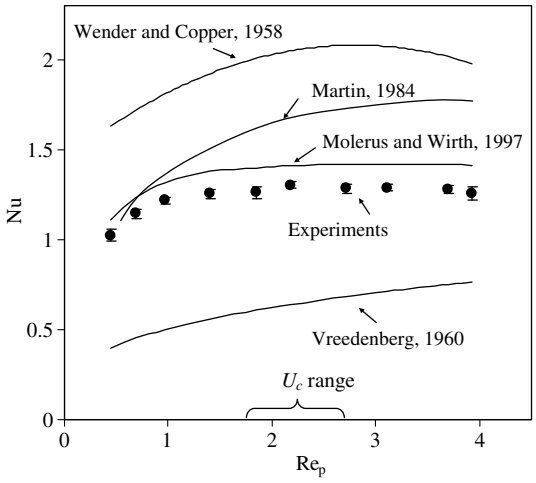

Fig. 3. Dimensionless heat transfer coefficient vs. Re_p for $H_0 = 0.8$ m, $r/R = 0$, $z = 0.6$ m compared with empirical and semi-empirical correlations.

might be due to increased voidage at high superficial gas velocities in the centre of the column. As can be seen in Fig. 4a, where the bed expansion is plotted against increasing superficial gas velocity, for $U < U_c$ the bed gradually expanded as the gas velocity increased. Then its surface level dropped slightly in the region of the transition to turbulent regime. The decrease in the expanded bed height at the onset of turbulent fluidization is probably due to increased entrainment of particles and the inability of the solids return system to recirculate all the entrained particles to the bed. At $U > 0.8$ m/s the expanded bed height dropped, to a level close to the top of the heater (marked on Fig. 4a) leaving a small portion of the heater exposed to a high voidage and contributing to a reduced heat transfer coefficient for $U > 0.8$ m/s. The mean bed voidage is also plotted on Fig. 4. The voidage increased continuously with increasing gas velocity, increasing at a higher rate for $U > 0.8$ m/s (Fig. 4a). Fig. 4b shows the expanded bed height and the bed voidage for $H_0 = 1.2$ m.

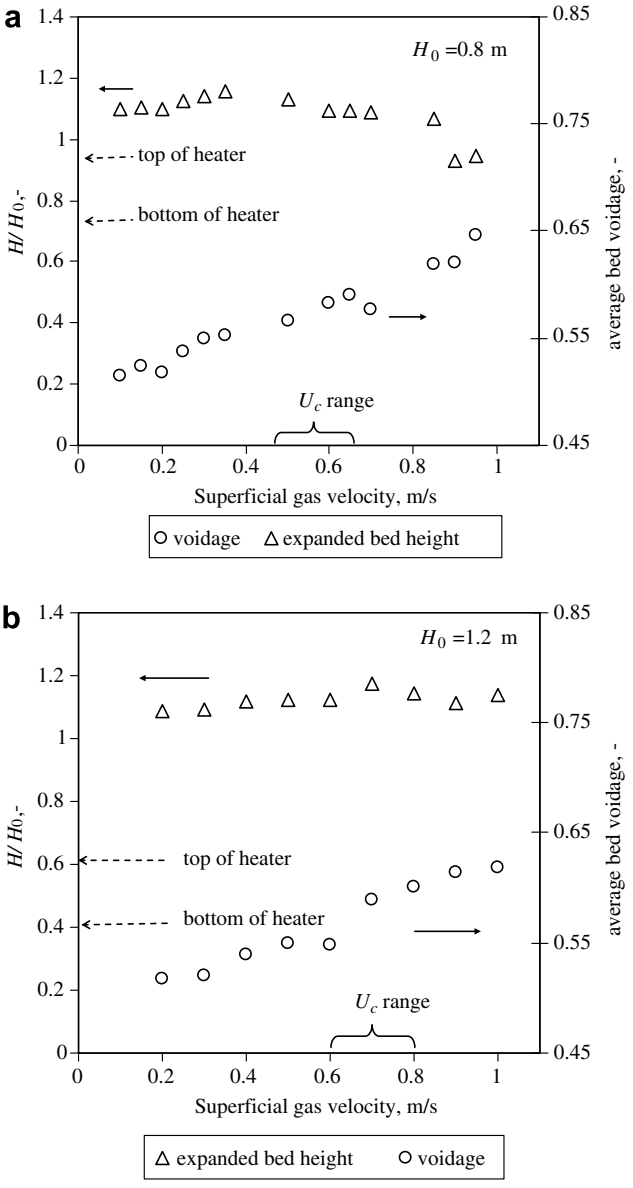

Fig. 4. Relative bed expansion and mean bed voidage for (a) $H_0 = 0.8$ m and (b) $H_0 = 1.2$ m.

For small particles, like those used in our experiments, the particle convection component is the dominant heat transfer mechanism. The frequency of exchange of particles at the surface and the particle concentration near the surface therefore play dominant roles. In bubbling beds, bubble behaviour determines the circulation patterns of particles, the frequency of exchange, and the time spent by particles at the surface. The particles travel mostly in the vertical direction, carried up in the bubble wakes, with their velocities depending on the velocity of the rising bubbles. Coalescence and splitting cause some lateral movement of the particles. The particles in the region close to the bed surface are accelerated by erupting bubbles, and then fall back onto the bed surface where they join the slow downwards-flowing dense phase near the walls and/or between bubbles. From the heat transfer point of view, the bigger, faster bubbles passing near the heating surface give higher heat transfer coefficients because they bring fast, "fresh" particles in their wakes. At the same time, they also expose the surface to more gas which exchanges and carries much less heat than the particles, but because larger bubbles also travel faster, they do not spend much time at the heater surface. The effect of increased voidage is overcome by the effect of increased particle exchange. The heat transfer coefficient continues to increase, despite the fact that the void fraction grows with increasing gas velocity. When the superficial gas velocity approaches the transition region, the increase of the heat transfer coefficient slows down, corresponding to the gradual change to the turbulent fluidization regime flow structure.

In the range of velocities corresponding to the onset of turbulent fluidization, the mechanism by which particles are exchanged at the heater surface begins to change as large bubbles become unstable and break up. Experimental

studies [18,19]) show that the flow structure is more homogenous, and it is difficult to distinguish between void and dense phase in the turbulent fluidization flow regime. Ellis et al. [19] reported that as the bed enters the turbulent flow regime the distribution of the measured local voidage is wider, as is the radial distribution of particle velocities. The magnitude of the measured particle velocity did not undergo a marked transition to the turbulent regime. Note that in their study the measurements were taken only in vertical direction, while by visual observation it is clear that there is increased lateral movement of particles in the turbulent flow regime. Hamidipour et al. [20,21] measured contact frequency and the axial distribution of particle contact times by means of a radioactive particle tracking technique. They found that for FCC particles the contact frequency was widely distributed in the turbulent flow regime and not significantly affected by increasing superficial gas velocity.

Bi et al. [22] suggested that bubble break-up is caused by transition to an open turbulent wake of a leading bubble when the void fraction in the bed is high and bubbles are separated by a critical distance from each other. Assuming that there is a critical Reynolds number, as proposed by Bi et al. [22], related to the maximum bubble diameter and a critical bubble velocity, beyond which vortex shedding occurs downstream of the rising bubble [23], we can postulate that detached vortices interact with each other and propagate through the bed like turbulent eddies. This causes a transition in the two-phase flow structure, carrying and accelerating particles from what used to be dense (emulsion) phase and entering the space occupied by distorted unstable voids. For this flow structure, fast particles contributing to the high heat transfer rates are brought to the heat exchange surface by detached vortices from the wake, or "turbulent eddies", that propagate independently, in contrast to the bubbling flow structure when wakes are closed and attached to the bubble. The heat transfer surface is exposed to a stream (mixture) of gas and particles with increased voidage which can come from any direction, spending very little time at the surface before being replaced by another stream. The lifespan of the eddies suspending the particles is expected to be short, as part of its turbulent energy is transformed into kinetic energy of the particles. The effect of increased voidage, which tends to decrease the heat transfer coefficients, is counterbalanced by the effect of increased frequency of particle exchange, in such a way that the heat transfer coefficients remain relatively unchanged with increasing gas velocity in the turbulent flow regime.

Fig. 3 compares our experimental data measured at the axis of 0.8 m deep bed, 0.6 m above the distributor, with published correlations and models. The effect of increasing gas velocity is captured very well by the Wender and Copper [24] correlation and the Molerus and Wirth [25] model. The latter gives the best predictions, with ~9% error. The error becomes larger (31%) at low gas velocities for a deeper bed ($H_0 = 1.2$ m), not shown on the figure. This approach is also unable to predict the effect of radial position in the bed. However, agreement with the experimental data is remarkably favourable. When the correlation constant in the Wender and Copper [24] equation is $Cr = 1$, the correlation gives ~56% error. For a correlation constant of $Cr = 0.62$ for $H_0 = 0.8$ m and $Cr = 0.75$ for $H_0 = 1.2$ m, this correlation fits the experimental data almost perfectly, with randomly distributed error in the range −3 to 7%. The Wender and Copper [24] correlation and Martin [26] model include voidage in their correlations. The mean bed voidage obtained experimentally was used in the calculations. The κ coefficient in the Martin [26] model was taken as 4, giving deviations from the experimental data from 0% to 40%, with the deviation increasing as the gas velocity increased. The correlation of Vreedenberg [27] under-predicts the heat transfer coefficient by 40–60% and does not follow the correct trend.

3.3. Effect of radial position

The behaviour of the heat transfer coefficient with increasing superficial gas velocity depends, as shown in Fig. 5, on the radial position of the heater, made dimensionless by the column radius (R), minus the radius of the heater tube, r_t, i.e. $R' = R - r_t$.

When the heater was located in the central region of the column, at lower superficial gas velocities the heater transfer coefficient increased, then went through a shallow maximum near the onset of turbulent fluidization regime, and finally slightly decreased in the turbulent regime, with increasing gas velocity, as explained above. For the heater locations $r/R' = 0.3$ and 0.6, the heat transfer coefficient remained relatively unchanged with increasing gas velocity once it reached the turbulent regime. As the heater approached the column wall the heat transfer coefficient increased with increasing gas velocity over almost the entire range of superficial gas velocities investigated, apparently slowing down after the transition to the turbulent

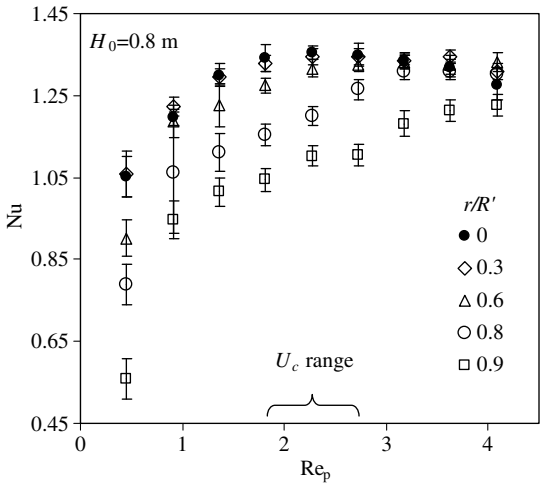

Fig. 5. Effect of heater radial location on Nu vs. Re_p profiles.

flow regime was complete. The different trend in the central region compared to the wall region can be attributed to the different flow structures in the two regions before the onset of the turbulent fluidization regime. The central region of the bed starts the transformation from a flow structure dominated by large fast-moving bubbles, whereas the region near the walls starts to transform from a dense layer of downward-moving mixture of gas and particles. Both regions gradually transformed towards a structure dominated by fast particles suspended in a stream of vigorously interacting turbulent eddies throughout the bed as the velocity increased.

For better illustration, the radial profiles of the measured heat transfer coefficients are shown on Fig. 6 for $H_0 = 0.8$ m. For $U < U_c$, the heat transfer coefficient increased at each radial location of the heater, giving flatter radial profiles as the gas superficial velocity increased. When the heater touched the column wall (i.e. $r/R' = 1$), channelling and gas bypassing were induced between the heater and the column wall, resulting in lower heat transfer coefficients. As the gas velocity increased beyond U_c, fluidization improved in this region. The bed appearance beyond U_c observed at the column wall was clearly turbulent, with streams of particles moving in all directions and unstable voids of irregular shape quickly appearing and disappearing. The slight asymmetry of the profile at $U = 0.1$ m/s might be due to uneven fluidization. The air distribution system was designed for high gas velocities, so the pressure drop at these low velocities was too low to assure uniform flow distribution across the bed cross-section. It was also difficult to set the gas flow to be precisely the same on different days when the two sides were done, and there were variations in relative humidity of the air.

When the gas superficial velocity exceeded U_c, the radial profiles of the heat transfer coefficient became flat and almost independent of increasing gas velocity. In the bubbling flow regime the maximum heat transfer coefficient in the radial profile can be attributed to increased bubble activity near the heater, bringing fresh particles to the surface, counterbalanced by increasing surface coverage by gas. Although the maximum voidage has been found in the centre of the bed in turbulent regime, and it increased with increasing gas velocity [19], the heat transfer coefficient remained relatively unchanged with increasing U. The small variation of the measured heat transfer coefficients is due to the coupled effects of increased frequency of particle exchange at the heater surface and increased voidage. In the turbulent fluidization regime the high heat transfer is due to the increased mixing because of the particles carried in the turbulent eddies, offsetting the effect of the increased voidage. For $U > 0.8$ m/s the heat transfer coefficient started to decrease slightly in the centre of the bed as particle entrainment increased and the effect of increased voidage become more influential.

3.4. Effect of static bed height

A set of experiments was performed where the heater was suspended at the same axial distance from the distributor plate ($z = 0.6$ m) and the same radial location in the column ($r/R = 0$) while the static bed height was varied. The results for the heater in the centre of the bed are given in Fig. 7. A transition in the heat transfer coefficient profiles was observed in the region of the onset to turbulent fluidization for all static bed heights investigated. For $H_0 = 1.0$ and 1.2 m with $H_0/D_t > 3$, the increasing bed depth did not have a significant effect on the heat transfer coefficient, nor on the onset of turbulent fluidization. There was about a 25% difference between the heat transfer coefficients measured in the 0.8 m and 1.2 m deep beds at low gas velocities, this difference diminishing as U increased beyond 0.6 m/s where there is a high probability that the bed was in the turbulent regime. Different circulation pat-

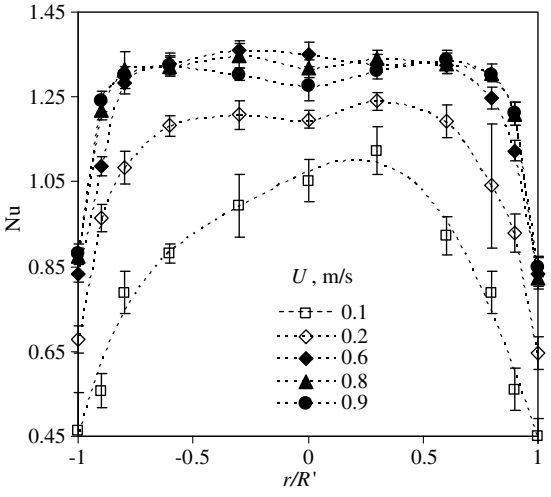

Fig. 6. Radial profiles of dimensionless time-mean heat transfer coefficient, $H_0 = 0.8$ m, $U_c = 0.46 \sim 0.65$ m/s.

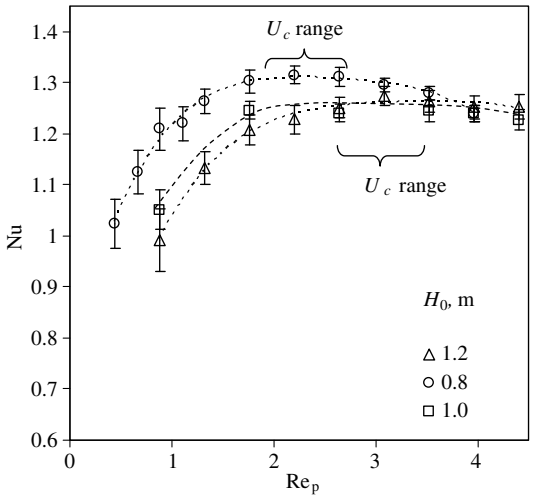

Fig. 7. Effect of bed depth on dimensionless time-mean heat transfer coefficients for tube in the centre of the bed.

terns [28] and proximity of the splash zone for $H_0 = 0.8$ m may explain the higher heat transfer coefficients in the bubbling regime. If we look at the distance from the top of the heater to the free bed surface, we see that for $H_0 = 0.8$ m the heater is in the top region of the bed, while for $H_0 = 1.2$ m the heater is in the middle of the bed. Stein et al. [29] reported increased particle velocities close to the free surface. This may have contributed to higher heat transfer rates at the bed axis for $H_0 = 0.8$ m for $U < U_c$.

The effect of the increased static bed height on the radial profiles of heat transfer coefficient is shown in Fig. 8. The open symbols represent data for $H_0 = 0.8$ m, whereas the bold symbols are for $H_0 = 1.2$ m. For $U < U_c$, slightly lower heat transfer coefficients were found in the centre of the bed with increased height, whereas slightly higher heat transfer coefficients were found towards the wall. The effect of increased static bed height on heat transfer undoubtedly depends on the void circulation patterns in the bed for lower gas velocities. Beyond the onset of the turbulent flow regime, the effect of the increased bed depth became negligible.

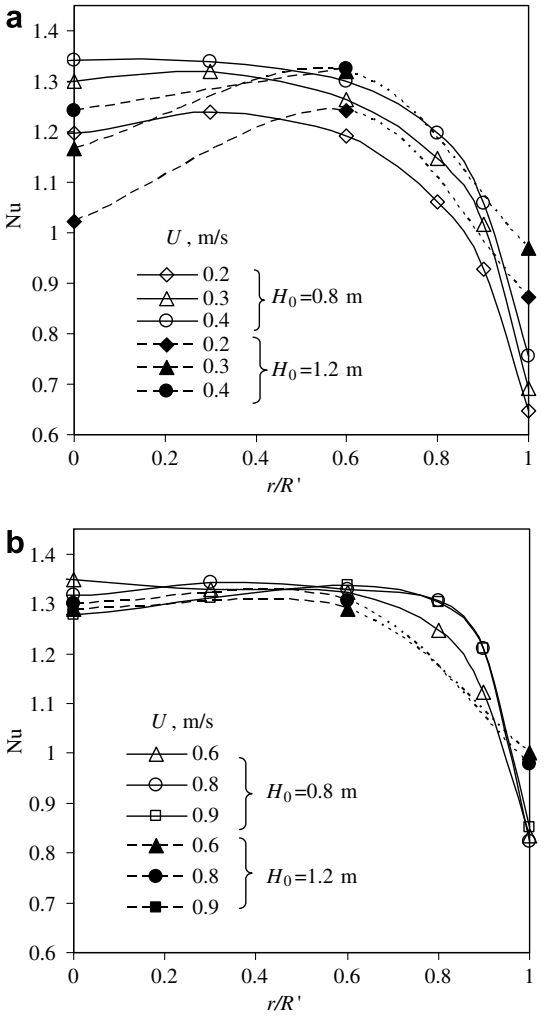

Fig. 8. Effect of static bed height on radial *Nu* profiles for (a) $U < U_c$ and (b) $U > U_c$.

4. Conclusions

For the conditions under which the experiments were carried out:

- Heat transfer coefficients were highest for $U \geqslant U_c$, and they changed very little in the turbulent flow regime, as long as the heater remained completely covered by dense bed.
- The radial profiles of the heat transfer coefficient were flat and not affected by increasing superficial gas velocity in the turbulent fluidization flow regime.
- The static bed height affected the heat transfer coefficients for $U < U_c$ due to the different circulation patterns in the bed for different static bed heights; this effect diminished with increasing U beyond U_c.
- The Molerus and Wirth [25] semi-empirical correlation gave the best predictions for our experimental results, with a 9% error for $H_0 = 0.8$ m and 11–31% error for $H_0 = 1.2$ m.

For $U < U_c$, the heat transfer coefficient is enhanced by the increased particle exchange at the surface caused by bubble wakes, while for $U > U_c$, the heat transfer coefficient is counterbalanced by the effect of increased voidage and increased frequency of particle exchange at the surface. In the turbulent flow regime, distinct dense and void phases no longer exist, and instead of bubble wakes, the particles are carried and accelerated by turbulent eddies initially created by vortex shedding downstream of the bubble when its rise velocity reaches a critical value. These turbulent eddies interact vigorously with each other, contributing to increased mixing and a more homogenous flow structure as the superficial gas velocity is increased. The transition to such a flow structure is gradual with increasing gas velocity, and any model describing the heat transfer across the different fluidization flow regimes should consider the gradual nature of the transition. Further hydrodynamic studies at the heat exchanger surface are needed to be able to further delineate the mechanism of particle exchange at the heater surface in the turbulent fluidization regime.

Acknowledgement

The authors thank the Natural Sciences and Engineering Research Council of Canada for their financial support.

References

[1] J.S.M. Botterill, Y. Teoman, K.R. Yuregir, Temperature effects on the heat transfer behaviour of gas fluidized beds, AIChE Symp. Ser. 77 (1981) 330–340.
[2] H.T. Bi, N. Ellis, I.A. Abba, J.R. Grace, State-of-the-art review of gas-solid turbulent fluidization, Chem. Eng. Sci. 55 (2000) 4789–4825.
[3] D. Kunii, O. Levenspiel, Fluidization Engineering, 2nd ed., Butterworth-Heinemann, Boston, 1991.

[4] I.A. Abba, J.R. Grace, H.T. Bi, M.L. Thompson, Spanning the flow regimes: Generic fluidized-bed reactor model, AIChE J. 49 (2003) 1838–1848.
[5] J.C. Chen, Heat transfer in fluidized beds, in: W. Yang (Ed.), Handbook of Fluidization and Fluid–Particle Systems, Marcel Dekker, New York, 2003, pp. 257–286.
[6] J.C. Chen, J.R. Grace, M.R. Golriz, Heat transfer in fluidized beds: Design methods, Powder Technol. 150 (2005) 123–132.
[7] P. Basu, P.K. Halder, P.K. Nag, Heat transfer in turbulent fluidized beds, in: Heat Transfer 1986, Proceedings of the 8th International Heat Transfer Conference, 1986, pp. 2599–2603.
[8] O. Hashimoto, S. Mori, S. Hiraoka, I. Yamada, T. Kojima, K. Tsuji, Heat transfer to the surface of vertical tubes in the freeboard of a turbulent fluidized bed, Int. Chem. Eng. 30 (1990) 254–258.
[9] A.C. Ku, M. Kuwata, F.W. Staub, Heat transfer to horizontal tube banks in a turbulent fluidized bed of large particles, AIChE Symp. Ser. 77 (208) (1981) 359–367.
[10] L. Leu, Y.K. Hsia, C.C. Chen, Wall-to-bed heat transfer in a turbulent fluidized bed, AIChE Symp. Ser. 93 (317) (1997) 83–86.
[11] F.W. Staub, Solids circulation in turbulent fluidized beds and heat transfer to immersed tube banks, J. Heat Transfer 101 (1979) 391–396.
[12] F.W. Staub, Flow and heat transfer in large particle turbulent fluidized beds, Proc. CIESC/AIChE Joint Meeting Chem. Eng. 1 (1982) 392–400.
[13] G. Sun, G. Chen, Transition to turbulent fluidization and its prediction, in: J.R. Grace, L.W. Shemilt, M.A. Bergougnou (Ed.), Fluidization VI, Engineering Foundation, New York, 1989, pp. 33–40.
[14] F.P. Incropera, D.P. DeWitt, Fundamentals of Heat and Mass Transfer, 5th ed., Wiley, New York, 2002.
[15] H.W. Coleman, W.G. Steele, Experimentation and Uncertainty Analysis for Engineers, second ed., Wiley, New York, 1998.
[16] A. Chen, H.T. Bi, Pressure fluctuations and transition from bubbling to turbulent fluidization, Powder Technol. 133 (2003) 237–246.
[17] N. Ellis, Hydrodynamics of gas–solid turbulent fluidized beds. Ph.D. dissertation, University of British Columbia, 2003.
[18] N. Mostoufi, J. Chaouki, Flow structure of the solids in gas-solid fluidized beds, Chem. Eng. Sci. 59 (2004) 4217–4227.
[19] N. Ellis, H.T. Bi, C.J. Lim, J.R. Grace, Hydrodynamics of turbulent fluidized beds of different diameters, Powder Technol. 141 (2004) 124–136.
[20] M. Hamidipour, N. Mostoufi, R. Sotudeh-Gharebagh, J. Chaouki, Experimental investigation of particle contact time at the wall of gas fluidized beds, Chem. Eng. Sci. 60 (2005) 4349–4357.
[21] M. Hamidipour, N. Mostoufi, R. Sotudeh-Gharebagh, J. Chaouki, Monitoring the particle-wall contact in a gas fluidized bed by RPT, Powder Technol. 153 (2005) 119–126.
[22] H.T. Bi, J.R. Grace, K.S. Lim, Transition from bubbling to turbulent fluidization, Ind. Eng. Chem. Res. 34 (1995) 4003–4008.
[23] R. Clift, J.R. Grace, M.E. Weber, Bubbles Drops and Particles, Academic Press, New York, 1978.
[24] L. Wender, G.T. Cooper, Heat transfer between fluidized solids beds and boundary surfaces – Correlation of data, Chem. Eng. Progr. 4 (1958) 15–23.
[25] O. Molerus, K. Wirth, Heat Transfer in Fluidized Beds, Chapman & Hall, New York, 1997.
[26] H. Martin, Heat transfer between gas fluidized beds of solid particles and the surfaces of immersed heat exchanger elements, part I, Chem. Eng. Process. 18 (1984) 157–169.
[27] H.A. Vreedenberg, Heat transfer between fluidized bed and vertical tube, Chem. Eng. Sci. 11 (1960) 274–285.
[28] A. Mathur, S.C. Saxena, A. Chao, Heat transfer from an immersed vertical tube in a gas-fluidized bed, Industrial & Engineering Chemistry, Process Des. Develop. 25 (1986) 156–163.
[29] M. Stein, Y.L. Ding, J.P.K. Seville, D.J. Parker, Solids motion in bubbling gas fluidized beds, Chem. Eng. Sci. 55 (2000) 5291–5300.